Chapter 3
Broadband Absorption of Microwaves in Periodic Cylindrical Structures

Lilit Gevorgyan, Henrik A. Parsamyan, and Hovhannes Haroyan

Abstract The absorption efficiency of a subwavelength conductive wire can be essentially increased in the broad microwave spectrum from 4 to 12 GHz by the appropriate choice of the radius and height of a wire. Such functional dependence ensures matching between the configuration and the incident field oriented by the wire axis. Theoretical results obtained within the limits of electrostatic approximation and numerical calculations reveal that the absorption cross-section of a wire can exceed the geometrical one by about 10 times, whereas the scattering efficiency is negligibly small. Such properties allow one to achieve relatively high absorption of the incident wave by a system consisting of the wires periodically distributed on a flat surface.

3.1 Introduction

For many years, electromagnetic absorbers have been widely used in the field of electromagnetic compatibility, sensors, bolometers, solar energy harvesting, heat emitters and new passive cooling technologies [1–3]. Effective materials that shield and absorb microwave radiation, particularly in the 2−18 GHz radar frequency range, are required for different defense and aerospace applications, for example creation of "stealth" aircraft [4, 5] camouflaging military ground devices and units from radar surveillance, and the design of anechoic chambers. In this context, the research and development of radio-absorbing materials have become essential.

In order to control electromagnetic waves to eliminate interference between different devices in a wide frequency band from RF to millimeter-wave spectrum, high-efficiency electromagnetic wave absorbers are required. This has an important role in future 5G wireless networks [6].

L. Gevorgyan · H. A. Parsamyan · H. Haroyan (✉)
Department of Radiophysics, Yerevan State University, A. Manoogian 1, 0025 Yerevan, Armenia
e-mail: hharoyan@ysu.am

H. A. Parsamyan
Center for Nanoscience and Technology, Institute of Chemical Physics, NAS RA, P. Sevak 5/2, 0014 Yerevan, Armenia

D. Blaschke et al. (eds.), *Optics and Its Applications*, Springer Proceedings in Physics 281, https://doi.org/10.1007/978-3-031-11287-4_3

As wireless communication technology is advancing, electronic equipment becomes widely used in many fields, thus leading to an increase in electromagnetic pollution [7]. In this regard, microwave absorbers effectively absorb electromagnetic waves, lowering the effects of electromagnetic pollution.

Commonly, the absorbing principles in absorbent materials are mainly linked to the dielectric loss or the magnetic loss. Nevertheless, because of the impedance mismatching at broad frequency ranges, these absorbers hardly achieve ultra-wideband absorption [8, 9].

Many absorbers have been developed, however the main drawbacks include thickness and difficulty of broadband impedance matching to free space. An ideal absorber should enjoy the benefits of a lightweight, low thickness, cost-effectiveness, wide bandwidth and good processability. The operating bandwidth is one of the most challenging problems, because different applications mostly demand wide-bandwidth absorbers. Multilayer structures and lossy materials with a tapered shape are commonly used to obtain wider operating bandwidths. However, this may result in a bulk volume and high cost [4, 10].

Many attempts have focused on developing metamaterial/metasurface-based absorbers from the microwave band to optical band. Limited by the resonance property, the operating bandwidth of the perfect metamaterial absorber (PMA) is usually narrow. In microwave band PMAs [11], typically comprised of dielectric thin-films sandwiched by a metallic split-ring resonator and cutting wire, can show near 100% absorbance at the resonant frequency, but they generally exhibit a narrow absorption bandwidth.

In recent years, all-dielectric metamaterial absorbers, composed of traditional microwave absorbing materials have shown their unique potential in improving impedance matching in a wide frequency band. One can achieve impedance matching with the surrounding by varying specific structures in these absorbers. Otherwise, material properties such as plasma frequency can be modified according to the targeted operating frequency. It is challenging to improve the absorbance and the bandwidth simultaneously because of the fundamental trade-off between the operational bandwidth and the attainable absorption. Therefore, most of the broadband perfect absorption structures are based on near to 90% absorption, and by trying to obtain higher absorbance, the bandwidth will drop dramatically. Consequently, further research is needed for obtaining the broadband absorption structure with higher absorbance.

3.2 Theory

Let ε_1 be the dielectric permittivity of the medium of a prolate spheroid with semi-axes a, b and c (so that $a > b = c$) placed in the environment with a real dielectric constant ε_2. Within the limits of electrostatic approximation (the dimensions of the spheroid are much smaller than the incident wavelength in the surrounding), the total dipole moment of the prolate spheroid is determined by the relation [12]:

$$P_x = \frac{ab^2}{3} \frac{\varepsilon_1 - \varepsilon_2}{\varepsilon_2 + (\varepsilon_1 - \varepsilon_2) n^{(x)}} E_x, \tag{3.1}$$

where

$$n^{(x)} = \frac{1 - e^2}{e^3} (\operatorname{arctanh} e - 1), \, e = \sqrt{1 - \frac{b^2}{a^2}}. \tag{3.2}$$

In the investigated case, when $b \ll a$, we have [13]:

$$n^{(x)} \approx \frac{b^2}{a^2} \ln \frac{2a}{2.7b}. \tag{3.3}$$

Henceforth, we will assume that the medium of the spheroid is a lossy material with the complex dielectric permittivity $\varepsilon_1 = \varepsilon_{1r} + i \cdot \varepsilon_{1i}$. Within the range of electrostatic approximation, the absorption and scattering cross-sections of the prolate spheroid are as follows:

$$\sigma_{abs} = \frac{8\pi^2}{\lambda} \frac{a^3}{3 \ln \frac{2a}{2.7b}} \frac{\varepsilon_2 \eta_i}{(\varepsilon_2 + \eta_r)^2 + (\eta_i)^2}, \tag{3.4}$$

$$\sigma_{scat} = \frac{2^7 \pi^5}{3^4} \frac{a^6}{\lambda^4} \frac{1}{\left(\ln \frac{2a}{2.7b}\right)^2} \frac{(\eta_r)^2 + (\eta_i)^2}{(\varepsilon_2 + \eta_r)^2 + (\eta_i)^2}. \tag{3.5}$$

Here

$$\eta_r = (\varepsilon_{1r} - \varepsilon_2) \frac{b^2}{a^2} \ln \frac{2a}{2.7b}, \, \eta_i = \varepsilon_{1i} \frac{b^2}{a^2} \ln \frac{2a}{2.7b}. \tag{3.6}$$

and λ is the wavelength in the surrounding medium.

In order to quantitatively describe the absorption and scattering properties of the investigated configuration, we employ the absorption and scattering efficiency factors:

$$Q_{abs} = \frac{\sigma_{abs}}{S} \text{ and } Q_{scat} = \frac{\sigma_{scat}}{S}. \tag{3.7}$$

We consider the case when $\lambda \gg a \gg b$. Therefore under specific conditions (the real and imaginary parts of dielectric constant of wires materials are the same order $\sim$103 for the fixed geometry: $r = 20\,\mu\text{m}$, $L = 5\,\text{mm}$ within considered frequency range (4−12 GHz)), the scattering efficiency is negligible compared to the absorption.

3.3 Results and Discussion

Full-wave numerical analysis based on the finite element method (FEM) was conducted to reveal the dependence of the absorption properties of the geometrical parameters. To simplify the simulated geometry, prevent simulation model from memory overflow due to the high density of the meshes in narrow regions, the prolate spheroid was replaced by an equivalent cylindrical wire having radius r=b and height $L = 2a$, schematically illustrated in Fig. 3.1a. The wire is illuminated by ax-polarized plane wave propagating along the y-axis. Within all simulations, we will assume that the wire height $L = 5\,\text{mm}$.

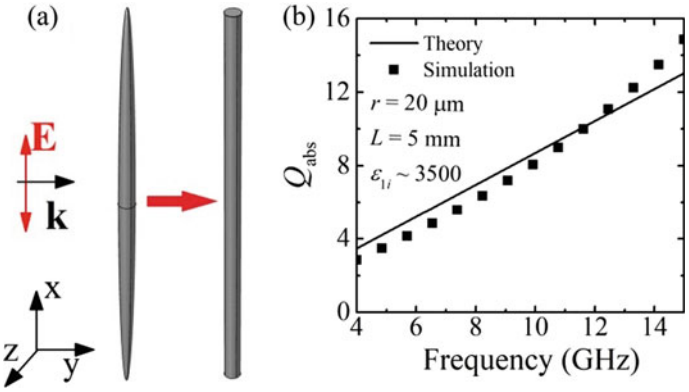

Fig. 3.1 **a** Schematic sketch of the prolate spheroid and the equivalent wire and **b** absorption efficiency spectra of the prolate spheroid obtained according to Eqs. (3.4) and (3.7) (solid line) and simulated (symbol). The sizes of the wire are for $r = 20\,\mu\text{m}$, $L = 5\,\text{mm}$, wire dielectric constant $\varepsilon_1 = \varepsilon_{1r} + i \cdot \varepsilon_{1i} = 1000 + i \cdot 3500$. The surrounding medium is air with $\varepsilon_2 = 1$

Figure 3.1b shows the theoretical (lines) and simulated (symbols) efficiency factor of the absorption for $r = 20\,\mu\text{m}$, $L = 5\,\text{mm}$, wire material dielectric constant is $\varepsilon_1 = \varepsilon_{1r} + i \cdot \varepsilon_{1i} = 1000 + i \cdot 3500$, which can be obtained by composite materials like graphite mixtures. The surrounding medium is air with $\varepsilon_2 = 1$. One sees that the theoretical results of the absorption efficiency for a prolate spheroid and simulations for an equivalent wire are rather in good agreement. Both numerical and theoretical analyses show that the absorption efficiency of the structures linearly depends on the frequency and increases for higher frequencies reaching to about 13 (Fig. 3.1b). However, the small mismatch of the numerical and theoretical results appearing at higher frequencies is the result of neglecting the quadrupole effects in the theoretical analysis.

To realize the absorption metasurface the periodical structure of appropriate distributed rods (wires) can be used. In this case, a trade off rod spacing should be chosen to minimize interaction, thereby reducing incident wave reflections without a large transition coefficient. In Fig. 3.2 is shown the geometry of the simulation, consisting

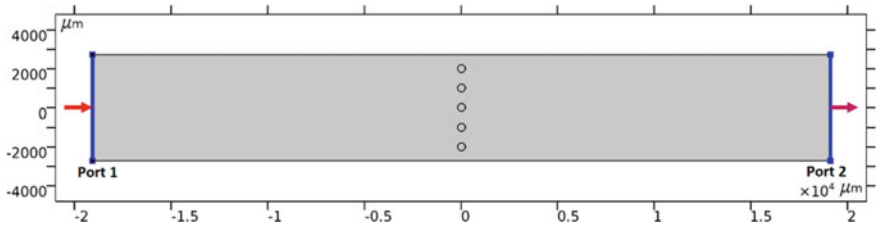

Fig. 3.2 Modeling geometry for one layer

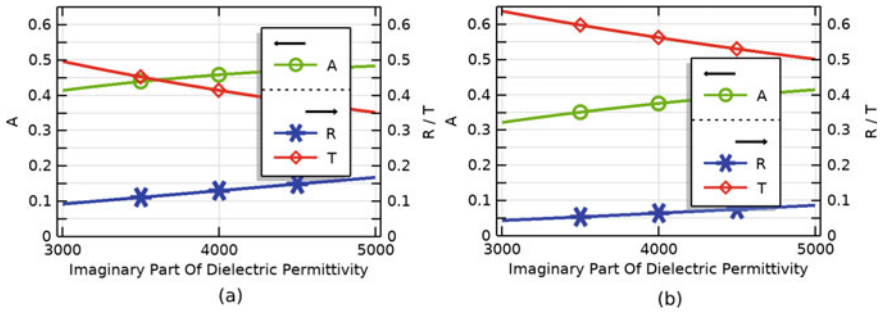

Fig. 3.3 Dependency of the reflection (asterisk), absorption (circle) and transmission (diamond) coefficients from the imaginary part of the dielectric permittivity, consisting of one layer of infinite rods, with parameters $r = 20\,\mu\text{m}$, $\varepsilon_r = 1000$, $f = 11\,\text{GHz}$. The distance between the two elements were **a** 1 mm and **b** 2 mm

of one layer of periodically distributed rods at distance of 1000 μm from each other. The grey rectangle illustrates the simulation domain composed of orderly arranged cylinders placed in free space. The incident plane wave is excited and received using the port boundary condition (Port1 and Port2, respectively). Arrows show the propagation direction of the incident electromagnetic waves.

Figure 3.3 shows the change in the coefficients of reflection (asterisk), absorption (circle) and transmission (diamond) (respectively R, A and T) as a function of the imaginary part of dielectric constant of the rods with parameters $\varepsilon_{1r} = 1000$, $r = 20\,\mu\text{m}$, $L = 5\,\text{mm}$, $f = 11\,\text{GHz}$ with a distance between the two elements of 1 mm (Fig. 3.3a), and 2 mm (Fig. 3.3b). The absorption coefficient is calculated using the following expression $A = 1 - R_2 - T_2$, where $R = |S_{11}|^2$ and $T = |S_{21}|^2$ are the reflection coefficient and the transmission coefficients, respectively. It is seen that the distance between the elements affects the reflection and absorption coefficient of the absorber: in the case of 1 mm $A \sim 0.48$, $R \sim 0.16$, $T \sim 0.36$, and in the case of 2 mm, $A \sim 0.41$, $R \sim 0.07$, $T \sim 0.52$.

It should be noted that the weak dependence of A, R, T parameters on the imaginary part of the dielectric constant of a wire enables do not to have precision quantities of the mixture components of graphite mixture which makes easier the fabrication of such structures.

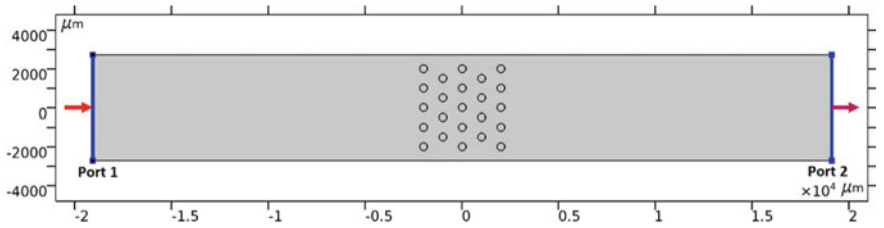

Fig. 3.4 Modeling geometry for five layers

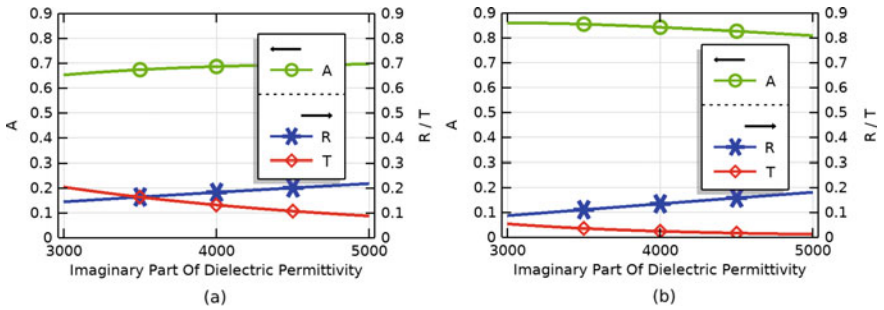

Fig. 3.5 Dependency of the reflection (asterisk), absorption (circle) and transmission (diamond) coefficients from the imaginary part of the dielectric permittivity of the absorber layers, the distance between the two elements of the layers were 1 mm. The distance between the layers were 1 mm (**a**), and 2 mm (**b**)

The efficiency of the absorption can be increased by creating an absorbing system consisting of multiple layers of such wires (Fig. 3.4).

The improvement of absorption feature of multilayer structure is clearly seen in Fig. 3.5. The dependence of the reflection (asterisk), absorption (circle) and transmission (diamond) coefficients on the imaginary part of the dielectric permittivity of the absorber wire, in the case of a five-layer structure presented in Fig. 3.5. The distance between two elements in one layer were 2 mm, $r = 20\,\mu\text{m}$, $\varepsilon_r = 1000$, $f = 11\,\text{GHz}$ **a** the distance between the layers 1 mm, **b** distance between layers 2 mm.

Further improvement of absorption can be reached by optimizing the distance between two nearby layers. To find the optimal distance between the layers, numerical analyses were carried out at different distances between the layers.

Figure 3.6 shows that increasing the distance between layers respectively increases the absorption coefficient and decreases the reflectance. However, at some point (in our case, from a distance of 10 mm), the absorption coefficient decreases.

To describe the dependency of absorption on the number of layers, the simulations were carried out by regularly adding the layers. Figure 3.7 shows that an increase in the number of layers leads to an increase in the absorption coefficient, but at some point (in our case from the 9th layer) the absorption coefficient becomes almost constant.

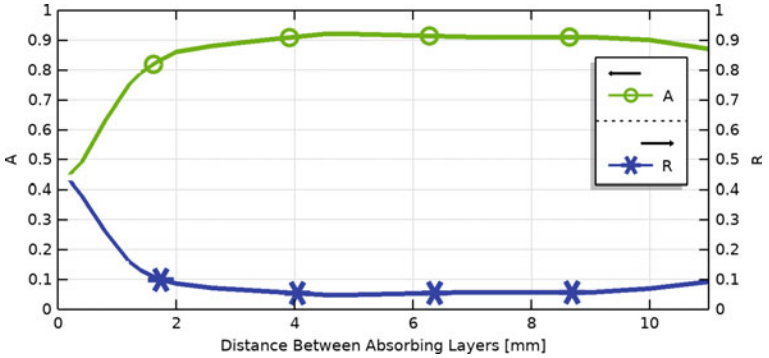

Fig. 3.6 Dependency of the reflection and absorption coefficients from the distance between the layers of a five-layer system

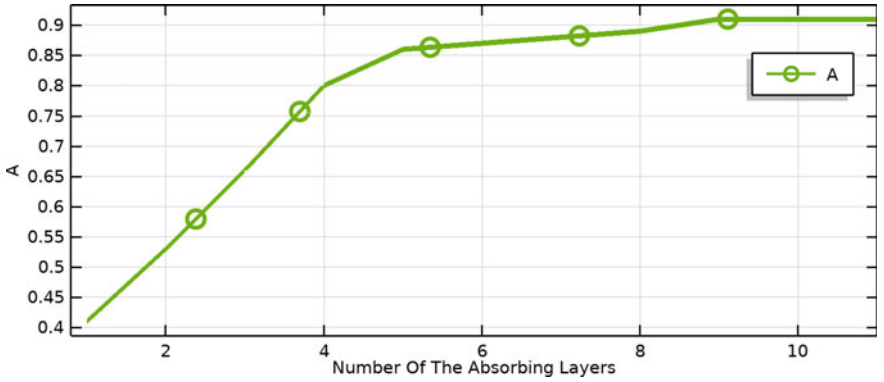

Fig. 3.7 Dependency of the absorption coefficient on the number of layers

As shown in Fig. 3.7, there is a significant increase in absorptance (0.85 and more) in the number of layers up to 5−7, after which the growth rate decreases sharply. This suggests that in practice, it is possible to not use too many layers, especially since an increase in the number of layers leads to an increase in the total thickness of the absorber. For example, in the case of having 5 layers, if the distance between the layers is 2 mm, the thickness of the system will be 1 cm, which, for example, at an operating frequency of 10 GHz is three times less than the wavelength.

The proposed structure is polarization-sensitive and it can absorb only linearly polarized incident field parallel to wires. This issue can be solved in a multilayer system by applying additional through one layers perpendicular to the initial ones.

Thus, depending on the formulation of the problem, it is possible to achieve different rates of absorption depending on the dielectric permittivity of the rods, their radius, the distance between them, and the distance between the layers.

3.4 Conclusion

Conductive subwavelength wires oriented to the polarization of the incident wave can serve as an effective basic element of broadband absorbers in the $4-12$ GHz microwave range. The absorption capacity of such absorbing rods can be significantly increased due to the correct choice of the geometrical and electrodynamics parameters of the structure. To obtain absorbing metasurfaces, periodic systems of absorber rods can be used, with which it is possible to provide surfaces with an absorption coefficient near 0.9. In particular, the results of numerical calculations show that the corresponding periodic arrangement of rods with a radius of $r = 20\,\mu$m, length $L = 5$ mm, $\varepsilon_1 = 1000 + i \cdot 3500$ can lead to broadband absorption of the order of 0.9, which is nearly uniform in a broad spectrum from 4 to 12 GHz.

Acknowledgements This work was supported by a scientific research grant through the Science Committee of MESCS of Armenia (20DP-1C05, 20APP-1C009,21AA-2B035and 21AG-1C061) and by a faculty research funding program 2021 implemented by Enterprise Incubator Foundation with the support of PMI Science.

References

1. Grant, J., Escorcia-Carranza, I., Li, C., McCrindle, I.J.H., Gough, J., Cumming, D.R.S.: A monolithic resonant terahertz sensor element comprising a metamaterial absorber and microbolometer. Laser Photon. Rev. **7**(6), 1043–1048 (2013)
2. Matsuno, Y., Sakurai, A.: Perfect infrared absorber and emitter based on a large-area metasurface. Opt. Mater. Express **7**(2), 618 (2017)
3. Raman, A.P., Anoma, M.A., Zhu, L., Rephaeli, E., Fan, S.: Passive radiative cooling below ambient air temperature under direct sunlight. Nature **515**(7528), 540–544 (2014)
4. Munk, B.: Frequency Selective Surfaces: Theory and Design, 1st edn. Wiley-Interscience, New York (2000)
5. Knott, E.F., Shaeffer, J.F., Tuley, M.T.: Radar Cross Section (Radar, Sonar and Navigation), 2nd edn. Scitech Publishing, New York (2004)
6. Rappaport, T.S., Xing, Y., MacCartney, G.R., Molisch, A.F., Mellios, E., Zhang, J.: Overview of millimeter wave communications for fifth-generation (5G) wireless networks - with a focus on propagation models. IEEE Trans. Antennas Propag. **65**(12), 6213–6230 (2017)
7. Liu, T., Pang, Y., Zhu, M., Kobayashi, S.: MicroporousCo@CoO nanoparticles with superior microwave absorption properties. Nanoscale **6**(4), 2447 (2014)
8. Peng, Z., Hwang, J.-Y., Andriese, M.: Absorber impedance matching in microwave heating. Appl. Phys. Express **5**(7), 077301 (2012)
9. Chen, X., Wu, Z., Zhang, Z., Heng, L., Wang, S., Zou, Y.: Impedance matching for omnidirectional and polarization insensitive broadband absorber based on carbonyl iron powders. J. Magn. Magn. Mater. **476**, 349–354 (2019)
10. Cui, Y., Fung, K.H., Xu, J., Ma, H., Jin, Y., He, S., Fang, N.X.: Nano Lett. **12**, 1443 (2012)
11. Tao, H., Landy, N.I., Bingham, C.M., Zhang, X., Averitt, R.D., Padilla, W.J.: Opt. Express **16**, 7181 (2008)
12. Landau, L.D., Pitaevskii, L.P., Lifshitz, E.M.: Electrodynamics of Continuous Media, 2nd edn. Elsevier Science & Technology, Oxford, United Kingdom (1984)
13. Solivérez, C.E. (eds.): Electrostatics and Magnetostatics of Polarized Ellipsoidal Bodies: The Depolarization Tensor Method. Free Scientific Information (2016)